

We are IntechOpen, the world's leading publisher of Open Access books Built by scientists, for scientists

4,800

Open access books available

122,000

International authors and editors

135M

Downloads

Our authors are among the

154

Countries delivered to

TOP 1%

most cited scientists

12.2%

Contributors from top 500 universities



WEB OF SCIENCE™

Selection of our books indexed in the Book Citation Index
in Web of Science™ Core Collection (BKCI)

Interested in publishing with us?
Contact book.department@intechopen.com

Numbers displayed above are based on latest data collected.
For more information visit www.intechopen.com



Stab Resistant Analysis of Body Armour Design Features Manufactured via Fused Deposition Modelling Process

Shajahan Maidin, See Ying Chong, Ting Kung Heing, Zulkeflee Abdullah and Rizal Alkahari

Abstract

Five designs of imbricate scale armour features for stab-resistant application were printed via fused deposition modelling process. Stab test on these designs against the HOSDB KR1-E1 stab-resistant body armour standard with impact energy of 24 Joules was conducted. The stab test was conducted on a number of samples measured thicknesses ranging from 4.0 to 10.0 mm by using Instron CEAST 9340 Drop Impact Tower to determine a minimum thickness that resulted in a knife penetration through the underside of sample which does not exceed the maximum penetration permissibility of 7.0 mm. Materials used for the samples were ABS-M30 and PC-ABS. Finally, one of the designs which offered the highest knife penetration resistance was selected. The results show that PC-ABS samples provide less shattering and lower overall knife penetration depth in comparison with ABS-M30. PC-ABS stab test demonstrated a minimum thickness of 8.0 mm, which was the most adequate to be used in the development of FDM manufactured body armour design features. Lastly, the design feature of D5 has shown to exhibit the highest resistance to the knife penetration due to the penetration depth of 3.02 mm, which was the lowest compared to other design features.

Keywords: fused deposition modelling, stab resistant, body armour, design features

1. Introduction

Sharp force injury is a common threat that police officers encounter since they involve in a wide range of duties from general, daily, patrol activities to specific criminal activities such as narcotic investigation [1, 2]. Stab resistant body armour has been increasingly used by the law enforcement and corrections officers in the European and Asian countries where more likely involve violent knife crimes due to tight restrictions on gun ownership [3].

In the United States, data released by the Federal Bureau of Investigation have shown that the law enforcement officers killed by handgun, rifle and shotgun occupied the highest percentage from 2005 to 2014 [4]. About 0.4% of the law enforcement officers were killed by knife or other cutting instruments, as compared

to other threats [4]. Despite the mortality rate caused by knife or other cutting tools was low, the stab resistant body armour has some practical and commercial experience in current service of the police forces [5].

The stab resistant body armour can be made from a range of materials, from traditional solutions, which are relatively heavy and provide little penetrate resistance, to the modern body armour made of ceramic, polycarbonate or aramid fibres which provide excellent stab protection, but are bulky, inflexible and uncomfortable to wear [6]. In an effort to reduce these limitations, the manufacture of stab resistant body armour must adhere to a series of internationally recognised test standards. According to the British HOSDB 2007 standard against knives and spikes, the knife should not penetrate more than 7 mm at the E1 press and 20 mm at the E2 press.

Besides, a number of studies were performed to reduce the weight of body armour and improve its flexibility. Stab resistance of modern armour was undoubtedly improved through implementation of modern standards, but historical issues such as comfort issues that causes thermal stress, poor fitting of armour hindering the body movement of wearers and affecting their work performance, etc. continue to exist with many of the current armour protection solutions [7, 8].

However, one of the alternative manufacturing technologies, the additive manufacturing (AM), has been increasingly implemented in a range of novel applications for customised clothing and high-performance textiles [9]. AM is an approach in which parts are designed in 3D CAD data and built by stacking material in layers [10]. AM technology allows the creation of complex geometries with reduced production time and cost, as well as the frequency of human intervention, which would be virtually difficult or impossible to produce via the traditional manufacturing processes such as injection moulding and milling. This technology presents an opportunity to design and develop novel solutions for conventional and high-performance textile applications because of their ability in generating geometric complexity and functionality as available from conventional fibre-based textiles [9]. Textile structures realised via AM techniques have received increasing attention since the previous decade. However, this solution is yet to be widely explored in an attempt to overcome the body armour issues. There are a range of AM techniques available in the market, including stereolithography apparatus (SLA), selective laser sintering (SLS), three-dimensional printing (3DP), and fused deposition modelling (FDM). However, FDM is the most widely used technique among these AM processes due to its simplicity and flexibility in manufacturing pure plastic parts with low cost, minimal wastage, and ease of material change [11, 12], which was first established by the Stratasys.

The world's first 3D conformal seamless AM textile garment was designed and manufactured by Bingham using Laser Sintering (LS) system [9]. The applications of AM textiles mostly via LS and 3D printer, especially in the field of fashion design, continue to increase. In addition, Johnson [13] attempted to address the issues that continue to exist with many current protective solutions in the body armour through AM. In their study, LS was adopted to develop stab resistant test samples for body armour. Browning [14] studied the structure of composite elasmoid type scales by measuring the mechanical response to blunt and penetrating indentation loading. In their study, additive manufactured model produced by using Fused Deposition Modelling technique was used only to mimic the feature of fish scale. However, there is no study about the creation of additive manufactured textiles via FDM system for stab resistant body protective armour with improved comfort ability and reduced weight.

2. Methodology

The aim of this research is to investigate the possibility of manufacturing stab resistant body armour samples via AM technology, specifically FDM. It is anticipated that the use of FDM can overcome the complexity in designing and manufacturing of stab resistant body armour, as well as reducing the weight and increasing the manoeuvrability of the body armour. The main objectives of the research are to investigate the feasibility of using FDM system to print the samples for stab resistance test; to design imbricated textile assembly with different design features; and to determine the results in terms of stab resistant performance under knife impact of 24 Joules according to the British HOSDB 2007 standard against knives and spikes impact.

2.1 Material used

Three stab tests were performed. Firstly, stab test was performed on planar samples measured thicknesses ranging from 4.0 to 6.0 mm, increasing in 1.0 mm increments fabricated with two different materials ABS-M30 and PC-ABS, respectively, in order to determine the most suitable material for the further stab resistance test and the stab resistant of this thickness range. Further stab test was performed on the selected material with higher range of thicknesses, which is from 7.0 to 10.0 mm, increasing in 1.0 mm increments mainly due to the previous thickness range that has failed to prevent the knife from being penetrated through the underside of the planar samples.

Furthermore, five different design features of the body armour were generated based on the combined knowledge of various design features which can be found in the natural biological body armour solutions such as animals and plants. In the end, one of the designs that provides the highest protection was selected—with the knife penetrated underneath the specimens was the lowest among all the designs. All five designs were designed mainly based on the inspiration of the hierarchal arrangement of elasmoid scales, which is regarded can offer high flexibility and provide multiple levels of protection to penetration [15, 16], as well as integrated with the design geometries of the other scales, as summarised in **Table 1**. Each scale assembly was formed via hinging connection features, which is inspired by the scale-based armour patents, in order to allow the scales to freely move among each other.

Table 2 shows the cross section of D1 which has been initially constructed with an assembly angle of 20° , while the individual scale thickness was 8.0 mm to ensure that minimum thickness established for the assembly was at least or not smaller than the minimum requirement of FDM printed sample—8.0 mm. Combining both thickness and assembly angle, a minimum cross-sectional thickness of 8.51 mm was achieved for D1. Scale thickness of D2 was reduced from 8.0 to 4.0 mm in an attempt to lower the total armour thickness and total assembly height of the following assemblies. Such reduction of scale thickness can be referred to the design features of elasmoid scales which informed that a scale thickness at the overlapping region is measured twice less than the thickness measured at the exposed region to form a multi-layered architecture [17]. To do this, the overlapping angle of individual scale element should be minimised to allow the formation of multi-layered overlapping layout. Browning [14] concluded that the scale armour featured imbricate scale assembly angle in between 10° and 20° able to offer higher flexibility and better protection due to the multi-layered structure and potentially to reduce back face deformation. The range of 10° – 20° assembly angle increasing 1° increments were therefore investigated, as shown in **Table 3**.

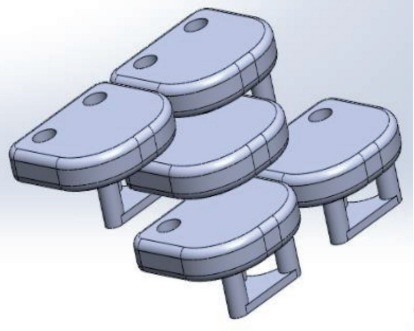
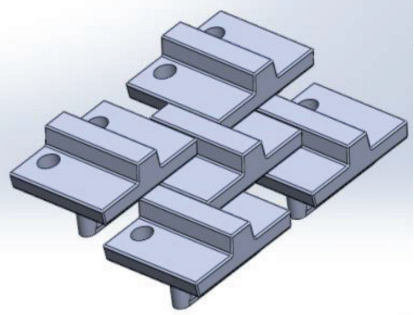
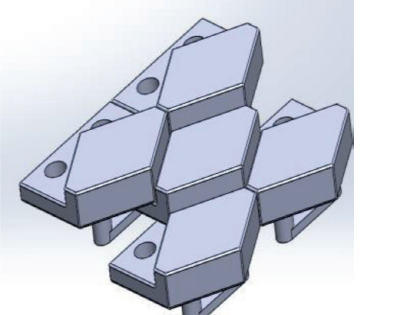
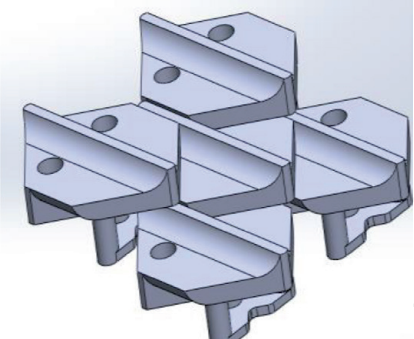
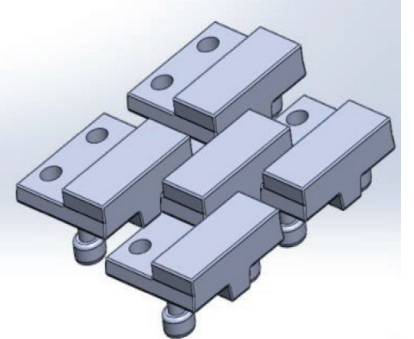
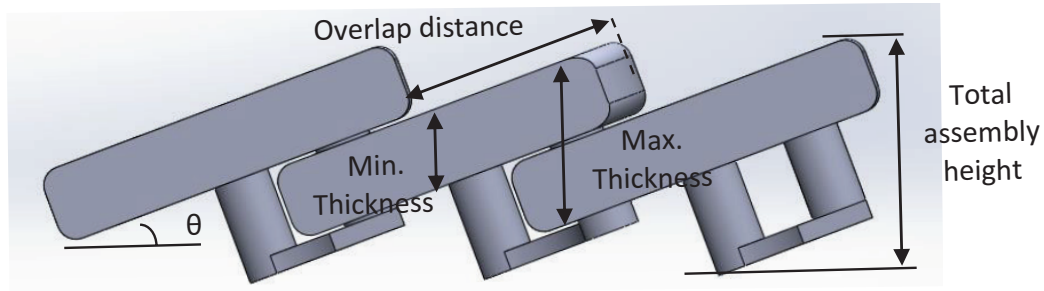
Design	Image	Description
D1		<p>This design was generated based on the inspiration that combined the design features of both the ancient Roman Lorica Squamata, which mimicked the design of natural elasmoid scale armour to allow a greater movement between the scale elements and potentially offer a high mobility to the wearer.</p>
D2		<p>This design was constructed with a thickness of 4.0 mm base scale element featuring a central protrusion along the top surface of each scale element, which is inspired by the geometric characteristic of the placoid and osteoderms. The purpose of using such structural feature was to eliminate the weakness found in between the overlapped scale elements.</p>
D3		<p>This design was created based on the design feature of elasmoid scale, which has different thicknesses at both overlapped and exposed regions. The exposed region of each planar scale was extruded with a hexagonal-shaped geometry from the top surface to encourage interlinking and manoeuvrability between individual elements and to assist in creating a multi-layered structure across the assembly.</p>
D4		<p>This design was designed with a thinner central protrusion along the top surface and gradually reducing closer to the edge of scales. Besides, an additional base plate extruded from the bottom of each scale element. Such design feature was inspired by combining the designs from both of the placoid scales and osteoderms, in order to eliminate the weakness found in between the overlapped scale element and, at the same time, to enhance the protective performance from all degrees.</p>
D5		<p>This design was designed in opposition to the idea of D4 by adding a wider central protrusion at the bottom part of each scale element and an additional rectangular plate on their top surfaces, in an attempt to resist the penetration of knife.</p>

Table 1.
Comparisons of five different design features.



Assembly angle, θ ($^{\circ}$)	Total assembly height (mm)	Overlap distance (mm)	Minimum thickness (mm)	Maximum thickness (mm)	Imbrications factor (K_d)
20	24.97	23.41	8.51	17.45	0.585

Table 2.
 Cross section of D1.

Assembly angle ($^{\circ}$)	Overlap distance (mm)	Minimum thickness (mm)	Maximum thickness (mm)	Imbrications factor (K_d)
20	12.09	11.34	13.62	0.302
19	12.78	8.88	13.54	0.320
18	13.54	8.83	13.46	0.339
17	14.39	8.78	13.38	0.360
16	15.34	8.74	13.33	0.384
15	16.42	8.70	13.25	0.411
14	17.65	8.66	13.19	0.441
13	19.06	8.62	8.62	0.465
12	20.70	4.09	8.59	0.518
11	22.64	4.07	8.56	0.566
10	24.95	4.06	8.53	0.624

Table 3.
 Investigation of assembly angle at 10–20 $^{\circ}$.

Based on the investigation of each assembly angle, the assembly angle that does not provide the imbricate scale assembly a minimum of 8.0 mm thickness or above will not be further considered in developing the other designs. **Table 3** highlights that a minimum thickness of 8.62 mm was obtained at the assembly angle of 13 $^{\circ}$, which fulfilled the requirement of minimum 8.0 mm thickness. The maximum thickness for the assembly overlapped at this angle was also established at a value of 8.62 mm. Besides, armour samples that designed with this assembly angle should be able to provide higher protection than D1 since the imbrication factor (K_d) was lower. **Figure 1** shows the section views of all designs, stab points, minimum thicknesses and total heights.

All the test samples were manufactured via Stratasys Fortus 400 MC which can provide higher quality of products. **Figure 2** shows the examples of PC-ABS material planar samples, and **Figure 3** shows the imbricate scale armour that was printed. It has to be noted that the creation of all designs must be considered on the FDM design guide to avoid part failure when building with FDM system. **Table 4**

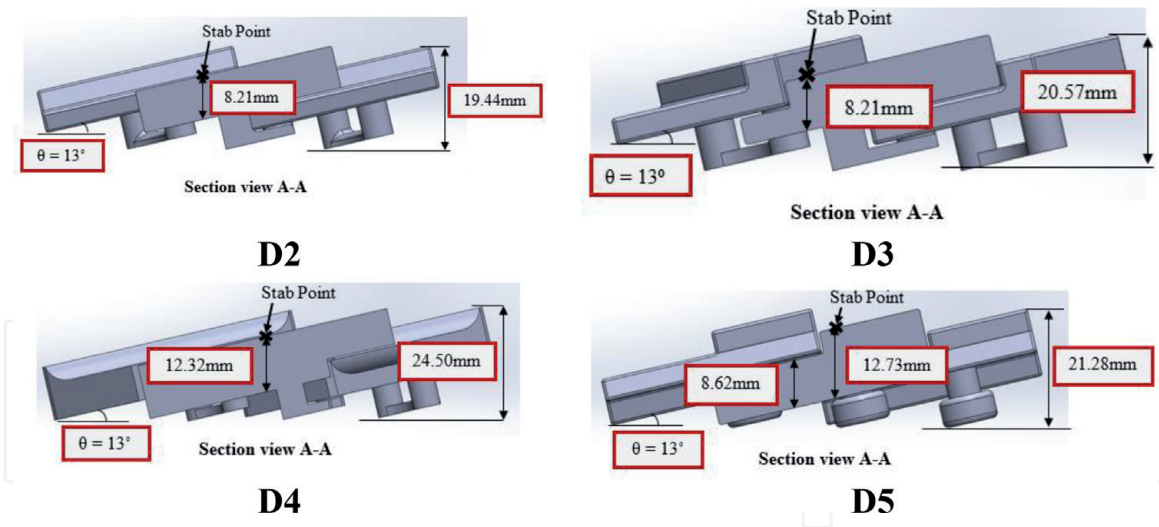


Figure 1.
Section view of all designs.

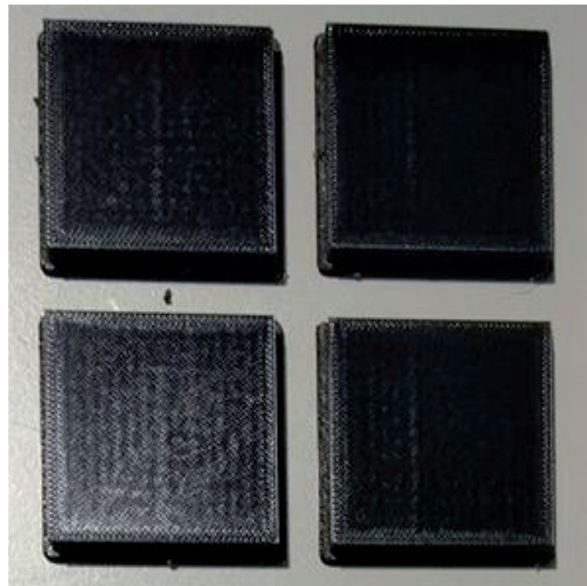


Figure 2.
Planar sample.

shows the process parameters used in printing the test samples. Both planar and imbricate test samples were printed with solid part interior fill to avoid from easily being penetrated by the knife. These samples were also built in 0° orientation and with wall thickness, that is, more than twice the layer thickness, in order to produce samples that have higher strength and impact resistance, and at the same time to minimise the height of printing which will affect the build time. However, build parameters such as raster angle, raster width and air gap, applied for both the materials were set to the default value.

Stab test was conducted using Instron CEAST 9340 Drop Tower (**Figure 4**) and securely installed with HOSDB standardised knife blade which dropped in the same direction of gravity during the stab test. By considering this, the stab test was performed at HOSDB KR1 with stab impact energy at E1 in the research; the acceptable blade penetration protruding through the underside of each test sample must not exceed a maximum penetration of 7.0 mm. In order to fulfil the requirements at this stab energy level, the parameters that include drop height and drop velocity need to be determined prior the stab test, as summarised in **Table 5**. Additionally, all these tests were conducted under an ambient temperature of 23°C with a relative humidity of 50%.

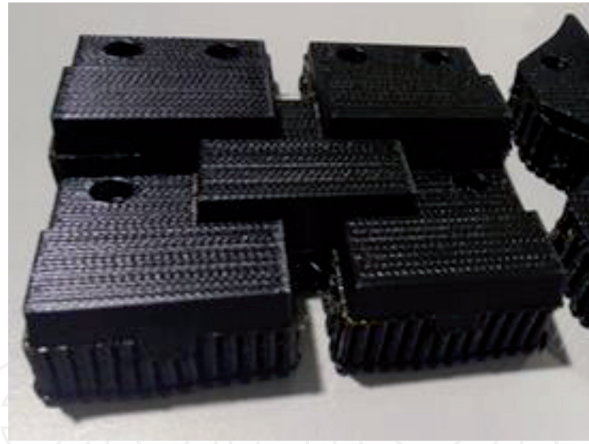


Figure 3.
Imbricate sample.

Parameters	Unit	ABS-M30	PC-ABS
Layer thickness	mm	0.254	0.254
Tip size	mm	T16	T16
Raster angle	°	45	45
Raster width	mm	0.014	0.014
Air gap	mm	0	0
Fill	%	100	100
Maximum build temperature	°C	325	335
Filament colour	—	white	black

Table 4.
Build parameters for ABS-M30 and PC-ABS materials.

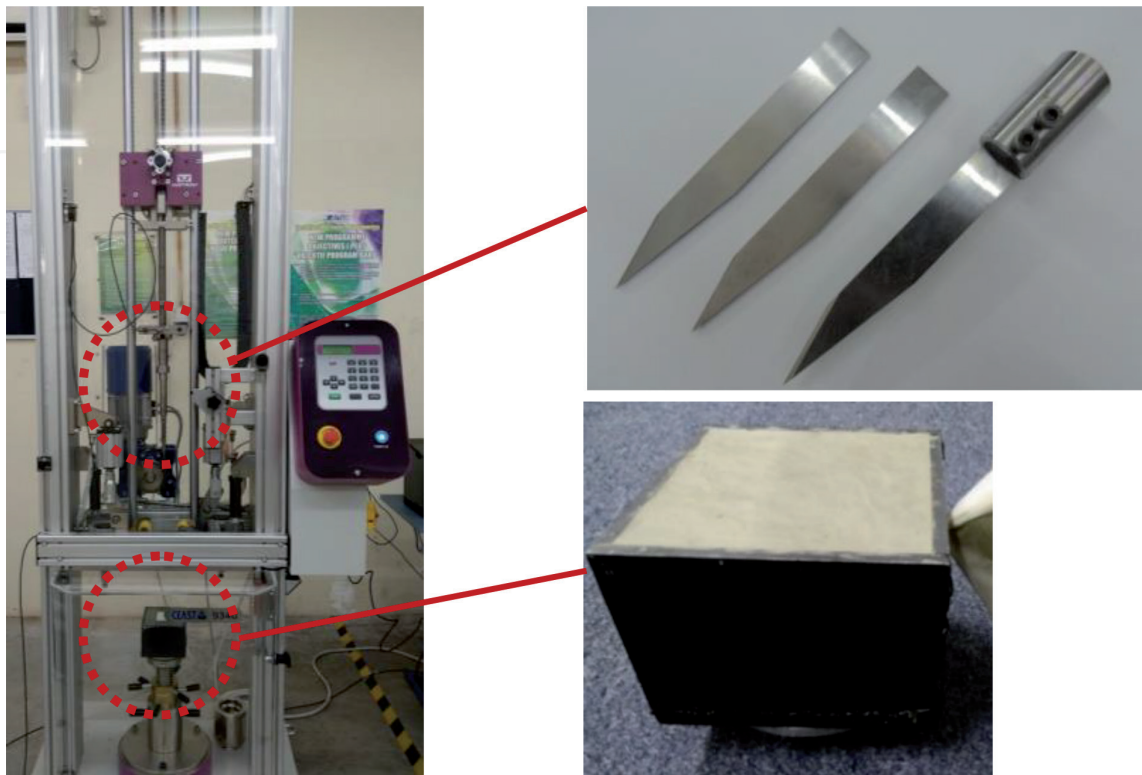


Figure 4.
Instron CEAST 9340 drop tower impact system.

Test requirements at KR1-E1	Units	Value settings
Stab impact energy	Joules	24 ± 0.5
Total drop mass	kg	3.226
Drop height	m	0.758
Drop velocity	m/s	3.86
Maximum blade penetration	mm	7.0

Table 5.
Experimental requirements of stab test at KR1-E1.

3. Results and discussion

Knife penetration depth occurred within the ABS-M30 and PC-ABS specimens measured with thickness groups ranging from 4.0 to 6.0 mm were significantly higher than the maximum allowable penetration of 7.0 mm, which indicates that this range was not suitable to be used for further armour designs. For ABS-30, samples measured with thicknesses of 4.0 and 5.0 mm were shattered into two pieces (**Figure 5**) and allowed a deep blade penetration into the backing clay. The measurement of knife penetration through the underside of these specimens was unpredictable since the samples were broken into pieces. However, the 5.00/3 sample was only punctured by the knife blade and caused a piece of small fragment broken from the underside of the specimen with a knife penetration depth of 20.10 mm, as documented in **Table 6**. The knife blade punctured through the 6.0 mm thick specimens does not cause any shatter to the sample, however the penetration depth occurred in the 6.00/3 sample was measured as 6.32 mm which has satisfied the allowable limit of knife penetration depth as defined in the HOSDB KR1-E1. The knife blade has pierced through the specimen and caused the underside

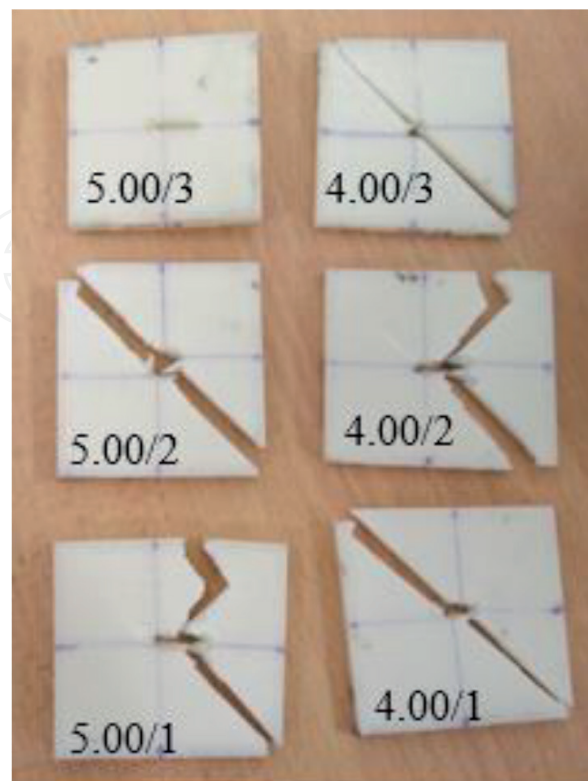


Figure 5.
Knife penetration of ABS test specimens.

Test	Specimen ID	Failure mode	Penetration depth (mm)	Result
1	6.00/1	Punctured	13.30	Fail
2	6.00/2	Punctured	9.65	Fail
3	6.00/3	Punctured	6.32	Pass
4	5.00/1	Shattered	—	Fail
5	5.00/2	Shattered	—	Fail
6	5.00/3	Punctured	20.10	Fail
7	4.00/1	Shattered	—	Fail
8	4.00/2	Shattered	—	Fail
9	4.00/3	Shattered	—	Fail

Table 6.
 Stab test result of ABS-M30 test specimens.

Test	Specimen ID	Failure mode	Penetration depth (mm)	Result
1	6.00/1	Punctured	14.96	Fail
2	6.00/2	Punctured	16.08	Fail
3	6.00/3	Punctured	15.23	Fail
4	5.00/1	Punctured	21.88	Fail
5	5.00/2	Punctured	20.06	Fail
6	5.00/3	Punctured	21.07	Fail
7	4.00/1	Punctured	39.40	Fail
8	4.00/2	Shattered	—	Fail
9	4.00/3	Shattered	—	Fail

Table 7.
 Stab test result of PC-ABS test specimens.

of specimen to crack from the stabbed region. However, it has to be noted that all the three 6.0 mm thick ABS-M30 specimens were forced deeply into the backing clay as compared to the other thickness group samples.

Table 7 shows the knife penetration depth measured from the underside surface of the PC-ABS planar samples measured thicknesses ranging from 4.0 to 6.0 mm. All samples failed to withstand the knife penetration since all the recorded penetration depth were higher than the maximum permissibility of 7.0 mm. However, total cases of shattering occurred in the PC-ABS were much less than the ABS-M30 since only two of the 4.0 mm thick PC-ABS samples (**Figure 6**) were shattered and demonstrated unmeasurable knife penetration.

Mean knife penetration depth of 6.0 mm thick ABS-M30 specimens was significantly lower than the PC-ABS specimens, with a difference of 5.67 mm, in spite of the mean knife penetrations occurred in both 6.0 mm thick ABS-M30 and PC-ABS samples were higher than the maximum permissibility of 7.0 mm. In that case, the stab resistance of the materials was further determined through the force/displacement traces of the impact event, and kinetic energy absorbed by the target samples measured 6.0 mm. **Figure 7** demonstrated the force/displacement traces of the impact event on the ABS-30 and PC-ABS target samples measured with thickness of 6.0 mm, respectively. The peak force values for the PC-ABS specimens in sequence order were approximately 0.992 kN, 0.918 kN and 0.987 kN, respectively, whereas

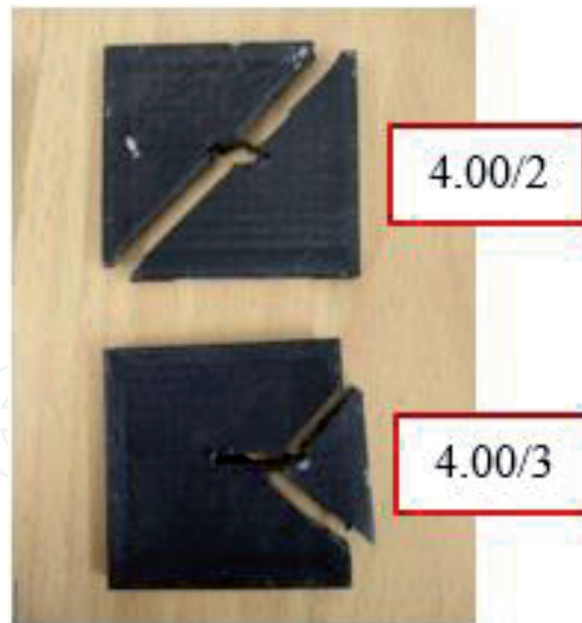


Figure 6.
Knife penetration of 4.00 mm test specimens.

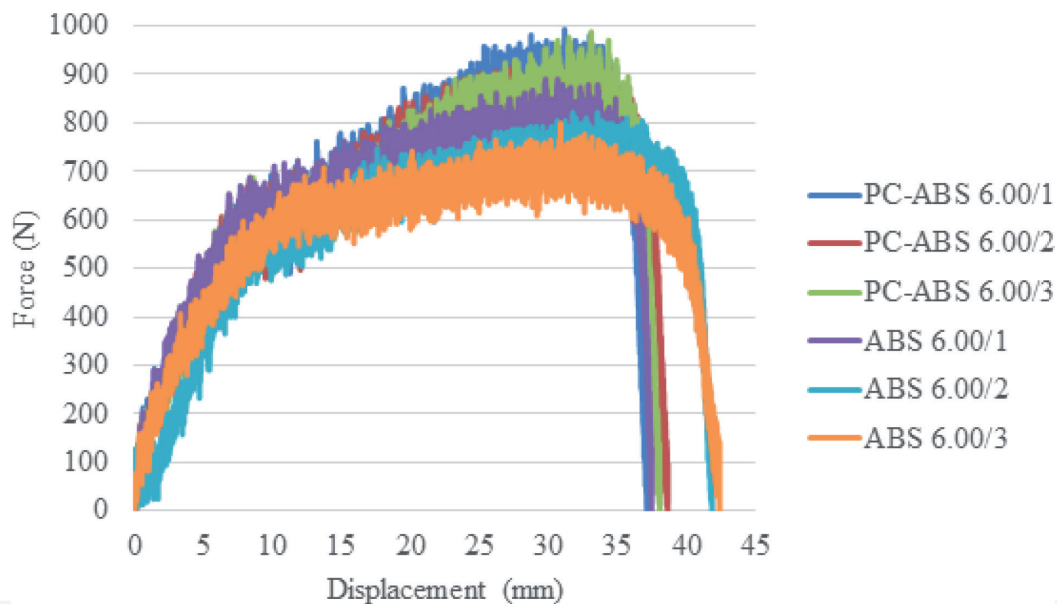


Figure 7.
Force/displacement traces.

the peak forces occurred in the ABS specimens were 0.890 kN, 0.822 kN and 0.800 kN, respectively. The force/displacement curves reveal that the maximum value of impact load where the failure of PC-ABS specimens began were higher than the ABS-M30 specimens. Besides, it can be also noted that the ABS-M30 specimens supported the load with longer displacement before completely penetrated as compared to the case of PC-ABS.

Impact damage in the FDM manufactured samples is caused by the loss of kinetic energy of the knife blade during penetration, so the energy absorption by the target specimens can be analysed using the formula, $E_{ab} = \frac{1}{2}m(v_i^2 - v_f^2)$, where E_{ab} is the energy absorbed by the target model during knife impact, m is the mass of the knife and v_i and v_f is referred to the initial and final velocity of the knife penetration [18]. **Figure 8** illustrated the energy absorbed by the ABS-M30 and PC-ABS specimens featured with 6.0 mm thickness group.

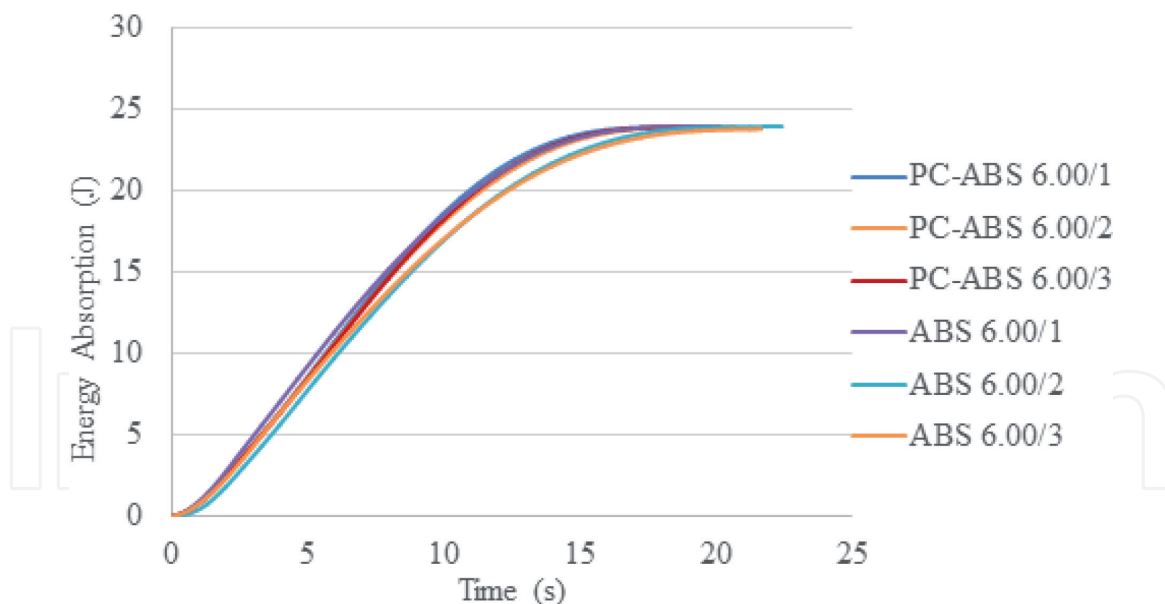


Figure 8.
Energy absorption by specimens measuring 6.00 mm thickness.

According to the trend shown in **Figure 8**, the ABS-M30 samples absorbed total energies of 23.967, 23.955 and 23.797 Joules, respectively, whereas the energy absorptions by the PC-ABS samples were 23.933, 23.950 and 23.948 Joules, respectively, which all were almost same as the available energy. Although the sample 6.00/1 of ABS-M30 material appeared to absorb higher stab impact energy than the PC-ABS samples, however, the overall mean energy absorption by the ABS-M30 specimens was slightly lower compared to the PC-ABS. On the whole, the PC-ABS tends to offer higher stab resistance performance than the ABS-M30 against the HOSDB KR1 E1 impact energy of 24 Joules. In addition, PC-ABS material tends to lock onto the knife blade to prevent it from being further penetrated, while the knife blade was also difficult to be released from the stabbed specimens. This can be attributed to the fracture toughness and impact resistance of PC-ABS; therefore, higher stab impact energy is required to pierce and deform it as compared to the ABS-M30 [19, 20].

PC-ABS planar specimens were then further constructed with thicknesses ranging from 7.0 to 10.0 mm and stab tested under the similar test conditions as previous experiment. The results obtained from this experiment were outlined within **Table 8**. Knife penetration through the underside surface of 7.0 mm thick PC-ABS samples was significantly higher than the maximum permissibility of 7.0 mm. However, the result obtained for 8.0 mm thick specimens was significantly reduced to an average depth of 5.47 mm which fulfilled the standard requirement. Furthermore, the samples measured thickness of 9.0 mm were only slightly punctured and resulted with a mean knife penetration depth of 2.24 mm. The samples measuring such thickness have demonstrated only one strike without knife punctured through the underside of the specimen. However, all of the 10.0 mm thick specimens resulted with no knife penetrated beyond the underside surfaces.

Figure 9 shows that the thickness of PC-ABS samples which was smaller than 8.0 mm provided lack of protection against the knife threat at this level, and it can be observed that the knife penetration depth was reduced as the thickness of samples increases, which indicates that the stab resistance increases as the thickness increases. Nevertheless, the thicknesses of 9.0 and 10.0 mm were not recommended to use for the further design activity of body armour via the FDM technique. Although these thicknesses provided higher stab resistance than

Test	Specimen ID	Failure mode	Penetration depth (mm)	Result
1	10.00/1	No failure	0.00	Pass
2	10.00/2	No failure	0.00	Pass
3	10.00/3	No failure	0.00	Pass
4	9.00/1	Punctured	3.83	Pass
5	9.00/2	Punctured	0.00	Pass
6	9.00/3	Punctured	2.89	Pass
7	8.00/1	Punctured	5.32	Pass
8	8.00/2	Punctured	5.24	Pass
9	8.00/3	Punctured	5.84	Pass
10	7.00/1	Punctured	12.01	Fail
11	7.00/2	Punctured	8.11	Fail
12	7.00/3	Punctured	10.45	Fail

Table 8.
Knife penetration depth of PC-ABS planar specimens.

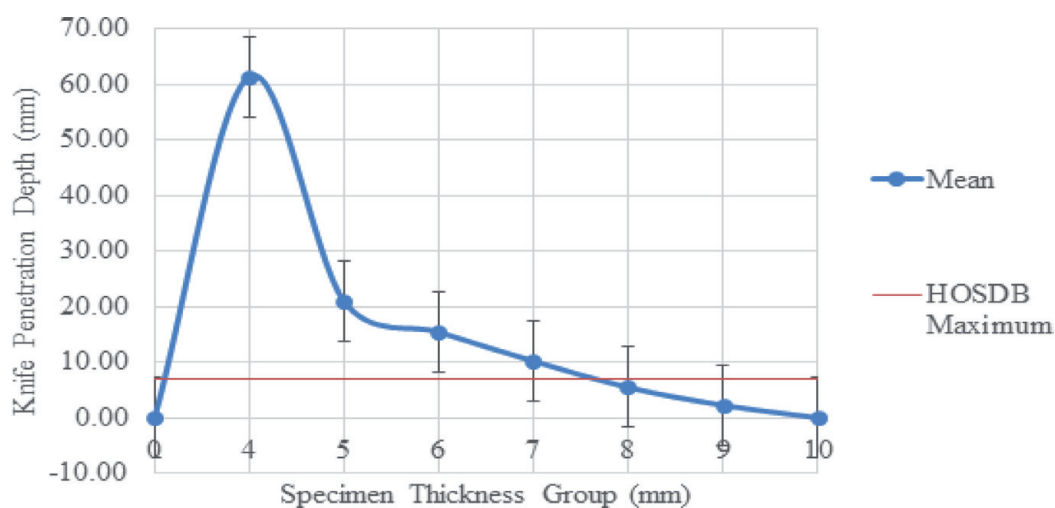


Figure 9.
Mean knife penetration depth per thickness group of PC-ABS planar specimens.

the thickness of 8.0 mm, but the concern was to avoid more weight added to the designs of body armour [21, 22]. Therefore, the 8.0 mm thickness was used as the minimum requirement in generating the designs of imbricate armour features.

Based on the result obtained in the stab test of the five designs, most of the stab tests demonstrated successful stab resistance which satisfied the requirement of lower than 7.0 mm, as defined within the HOSDB KR1-E1 impact energy of 24 Joules. However, the D2 and D3 demonstrated negative results to such level of impact energy, as demonstrated in **Figure 10**.

D3 offered the lowest stab resistance with a knife penetration depth which was the highest as compared to the other designs. The mean knife penetration depth was 12.08 mm which was larger than the HOSDB maximum penetration level. The minimum overlapping thickness where the knife punctured was the reason that caused the failure in D3 samples since it measured only 8.21 mm (**Figure 1**), which can be considered as the lowest measurement as compared to

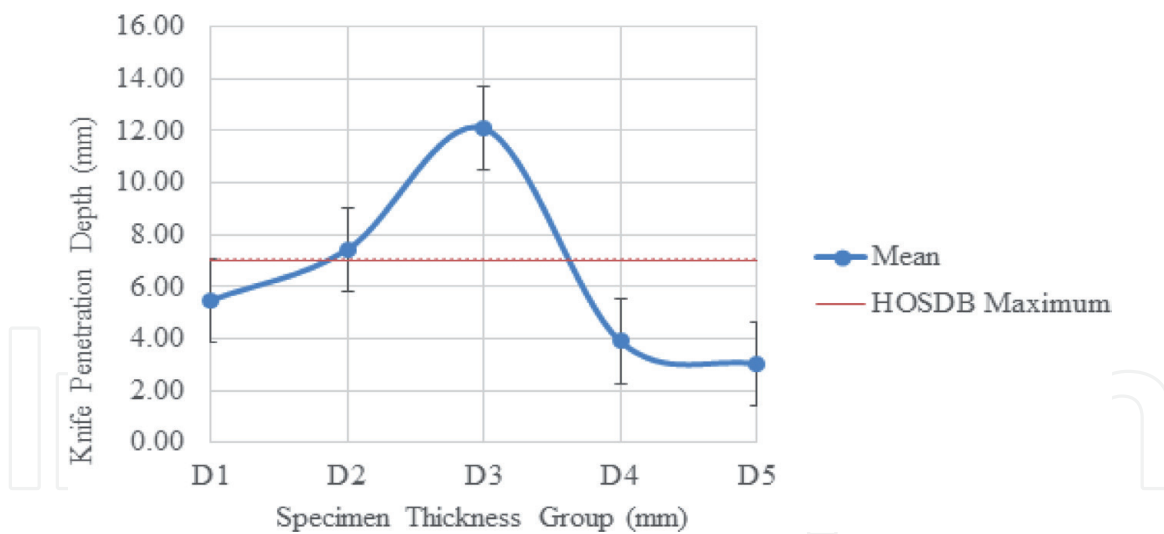


Figure 10.
Comparison of mean knife penetration depth of the design features.

other designs. Mean knife penetration depth resulted in D2 was 7.43 mm, which was lower than D3, but D2 did not effectively withstand the knife threat due to the knife penetration depth occurred in it was higher than 7.0 mm. On the other hand, D1, D4 and D5 demonstrated higher stab resistance to the HOSDB KR1-E1 impact energy. On the other hand, D1 provided acceptable level of protection with a mean knife penetration of 5.37 mm which was lower than 7.0 mm. However, this design was not as efficient as the designs of D4 and D5. This indicated that reduction in the total thickness of the imbricate structure will not reduce the stab resistance of the FDM-manufactured imbricate body armour, yet it can also provide more effective protection to the wearer from sustaining a life-threatening injury. Furthermore, D4 demonstrated stab resistance which was relatively lower than D5, since the mean knife penetration depth of the D4 specimens was 0.87 mm higher than that resulted in the D5 samples. **Figure 11** shows the test result of D4 specimen.

However, D5 samples demonstrated were most successful to withstand a knife threat to the HOSDB KR1 impact energy of 24 Joules since D5 has provided the highest stab resistance with a mean knife penetration depth of 3.02 mm which was the lowest as compared to the other designs. An individual scale was broken away from the D5 assembly as shown in **Figure 12** for illustration.

One of the reasons that causes the neighbour scale to be disconnected from the assembly was the design feature of assembly link which offered less effort to hold the scales tightly. Furthermore, the resistance between the knife blade and specimens has led to the formation of crack from the edges of the target scale. Despite one of the neighbour scales was disconnected from the assembly due to the impact of knife blade, the design feature of the assembly was able to lock the knife blade to resist further penetration into the structure of material. In addition, the stab resistance of the D5 will slightly reduce if the knife blade punctures at the front part which far away from the higher thickness region since thickness along the front part of sample was measured 8.62 mm (**Figure 1**). Despite the linkage failure occurred within D5 samples, the broken and loose pieces will be contained within the structure due to the overlapping nature of imbricate design. This may be not obviously seen in this experiment as the sample was not a complete body armour assembly. More importantly, this phenomenon has not resulted with knife penetration which is greater than the allowable limit of 7.0 mm and it was also the lowest among the designs.



Figure 11.
Stab test result of D4 specimen from (a) top and (b) bottom view.

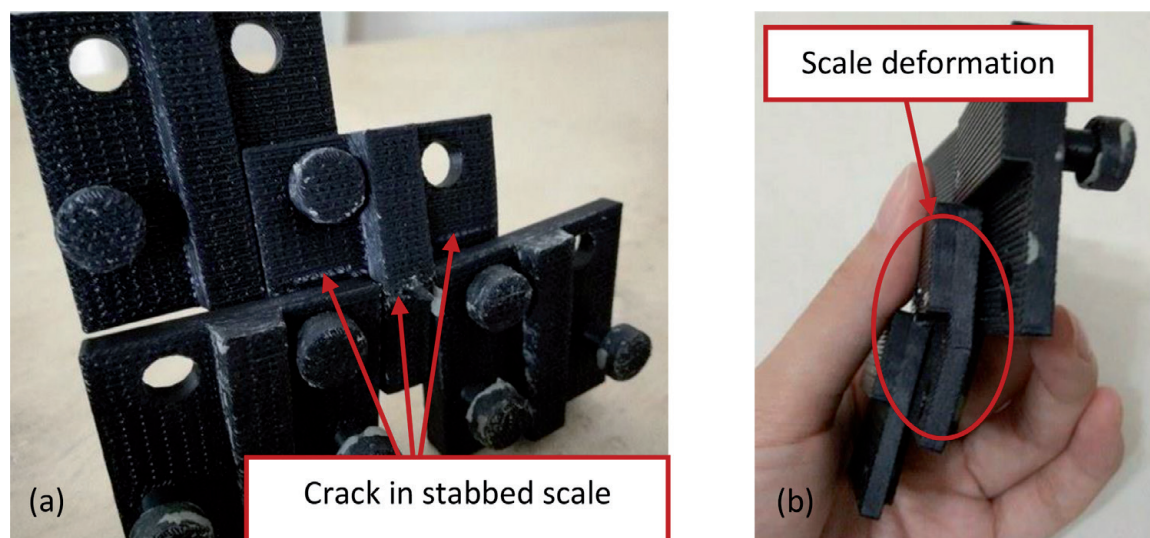


Figure 12.
Stab test result of D5 specimen from (a) bottom and (b) side view.

4. Conclusion

Stab experimental test was conducted on a range of planar specimens manufactured via Stratasys Fortus 400 MC system against HOSDB KR1-E1 impact energy of 24 Joules, to decide the selection of material and identify a minimum thickness of the FDM-manufactured specimens. It was important to identify the minimum thickness of the FDM-manufactured specimens for stab resistance, since the minimum thickness was necessary to provide a reference for the design of imbricate armour features. The result obtained in the stab test of the planar specimens demonstrated that the PC-ABS exhibited higher resistance to the knife blade due to the knife penetration depth that occurred in it was lower than the ABS-M30. Besides, less specimens manufactured from PC-ABS were shattered as compared with the PC-ABS; thus, the PC-ABS samples demonstrated higher levels of toughness and were therefore able to absorb the stab impact energy. Meanwhile, an optimum minimum thickness of 8.0 mm has been determined for specimens manufactured using PC-ABS. Although thicknesses of 9.0 and 10.0 mm have

shown greater stab resistance than the 8.0 mm specimens, these thicknesses should not be used to establish the imbricate armour design features since it can increase the weight of armour.

Result obtained from the stab test has shown that the D5 design features which adopted an extruded plate at the exposed region of overlapping scales and featured a central protrusion along the bottom of each scales demonstrated the highest stab resistance against the knife penetration with an impact energy of 24 Joules as compared to the other designs. The knife penetration depth measured from this design was only 3.02 mm. Despite one of the neighbour scales was disconnected from the assembly due to the impact of knife blade, the design feature of the assembly was able to lock the knife blade to resist further penetration into the structure of material.

Acknowledgements

We are grateful to all those who have assisted direct or indirectly to complete this study and appreciate financial support by Universiti Teknikal Malaysia Melaka.

IntechOpen

Author details

Shajahan Maidin*, See Ying Chong, Ting Kung Heing, Zulkeflee Abdullah
and Rizal Alkahari
Universiti Teknikal Malaysia Melaka, Hang Tuah Jaya, Melaka, Malaysia

*Address all correspondence to: shajahan@utem.edu.my

IntechOpen

© 2019 The Author(s). Licensee IntechOpen. This chapter is distributed under the terms of the Creative Commons Attribution License (<http://creativecommons.org/licenses/by/3.0>), which permits unrestricted use, distribution, and reproduction in any medium, provided the original work is properly cited. 

References

- [1] Parsons JRL. 'Occupational Health and Safety Issues of Police Officers in Canada, the United States and Europe: A Review Essay' [Online]. 2004. Available at: <https://www.mun.ca/safetynet/library/OHandS/OccupationalHS.pdf> [Accessed on: 15 May 2018]
- [2] National Institute of Justice. 'Stab Resistance of Personal Body Armor NIJ Standard-0115.00 (NCJ #183652). Rockville, MD: National Law Enforcement and Corrections Technology Center, U.S. Department of Justice; 2000
- [3] Hilal SM, Densley JA, Li SD, Ma Y. The routine of mass murder in China. *Homicide Studies*. 2014;**18**(1):83-104
- [4] Federal Bureau of Investigation. 2014 Preliminary Statistics for Law Enforcement Officers Killed and Assaulted [Online]. 2015. Available: <https://ucr.fbi.gov/leoka/2014>
- [5] Horsfall I. 'Stab resistant body armour' [Ph.D. dissertation]. Cranfield: Cranfield University; 2000
- [6] Egres Jr., RG, Decker MJ, Halbach CJ, Lee YS, Kirkwood JE, Kirkwood KM, et al. "Stab resistance of shear thickening fluid (STF) – Kevlar composites for bodyarmor applications". In: Proceedings of the 24th army science conference. Orlando, Florida; Nov. 29-Dec. 2. 2004
- [7] Stubbs D, David G, Woods V, Beards S. Problems associated with police equipment carriage with body armour, including driving. In: Proceedings of the International Conference on Contemporary Ergonomics (CE2008). Nottingham, UK; 1-3 April 2008
- [8] Xiong H. 'Police officers: Surviving a real life-threatening incident while wearing body armor' [Ph.D. thesis]. Stanislaus: California State University; 2014
- [9] Bingham GA, Hague RJM, Tuck CJ, Long AC, Crookston JJ, Sherburn MN. Rapid manufactured textiles. *International Journal of Computer Integrated Manufacturing*. 2007;**20**(1):96-105
- [10] Gibson I, Rosen D, Stucker B. *Additive Manufacturing Technologies: 3D Printing, Rapid Prototyping, and Direct Digital Manufacturing*. Berlin: Springer; 2014
- [11] Ning F, Cong W, Qiu J, Wei J, Wang S. Additive manufacturing of carbon fiber reinforced thermoplastic composites using fused deposition modeling. *Composites Part B: Engineering*. 2015;**80**:369-378
- [12] Chohan JS, Singh R. Pre and post processing techniques to improve surface characteristics of FDM parts: A state of art review and future applications. *Rapid Prototyping Journal*. 2017;**23**(3):495-513
- [13] Johnson A, Bingham GA, Wimpenny DI. Additive manufactured textiles for high performance stab resistant applications. *Rapid Prototyping Journal*. 2013;**19**(3):199-207
- [14] Browning A, Ortiz C, Boyce MC. Mechanics of composite elasmoid fish scale assemblies and their bioinspired analogues. *Journal of the Mechanical Behavior of Biomedical Materials*. 2013;**19**:75-86
- [15] Helfman GS, Collette BB, Facey DE, Bowen BW. *The Diversity of Fishes: Biology, Evolution, and Ecology*. 2nd ed. New Jersey: John Wiley & Sons; 2009
- [16] Zhu D, Ortega CF, Motamedi R, Szewciw L, Vernerey F, Barthelat F. Structure and mechanical

performance of a “Modern” fish scale.
Advanced Engineering Materials.
2012;**14**(4):B185-B194

[17] Lin YS, Wei CT, Olevsky EA, Meyers MA. Mechanical properties and the laminate structure of arapaima gigas scales. *Journal of the Mechanical Behavior of Biomedical Materials*. 2011;**4**(7):1145-1156

[18] Dhakal HN, Zhang ZY, Richardson MOW, Errajhi OAZ. The low velocity impact response of non-woven hemp fibre reinforced unsaturated polyester composites. *Composite Structures*. 2007;**81**(4):559-567

[19] Seelig T, Van der Giessen E. Effects of microstructure on crack tip fields and fracture toughness in PC/ABS polymer blends. *International Journal of Fracture*. 2007;**145**(3):205-222

[20] Stratasys. ‘FDM Thermoplastics Material Overview’ [Online]. 2017. Available at: <http://www.stratasys.com/materials/fdm> [Accessed: 11 May 2018]

[21] Potter AW, Karis AJ, Gonzalez JA. ‘Biophysical Characterization and Predicted Human Thermal Responses to US Army Body Armor Protection Levels (BAPL) (No. USARIEM-TR-T13-5)’. MA: U.S. Army Research Institute of Environmental Medicine. 2013

[22] Bossi LL, Jones ML, Kelly A, Tack DW. A Preliminary Investigation of the Effect of Protective Clothing Weight, Bulk and Stiffness on Combat Mobility Course Performance. *Proceedings of the Human Factors and Ergonomics Society Annual Meeting*. 2016;**60**(1):702-706